ESSA RESEARCH LABORATORIES
Air Resources Laboratories
Silver Spring, Maryland
February 1969

Results of Vertical-Velocity Fluctuation Measurements in the Atmospheric Boundary Layer Over a Salt-Hay Marsh

G.A. HERBERT
R.R. SOLLER

Technical Memorandum ERLTM-ARL 11
U.S. DEPARTMENT OF COMMERCE / ENVIRONMENTAL SCIENCE SERVICES ADMINISTRATION

A RESEARCH LABORATORIES

AIR RESOURCES LABORATORIES

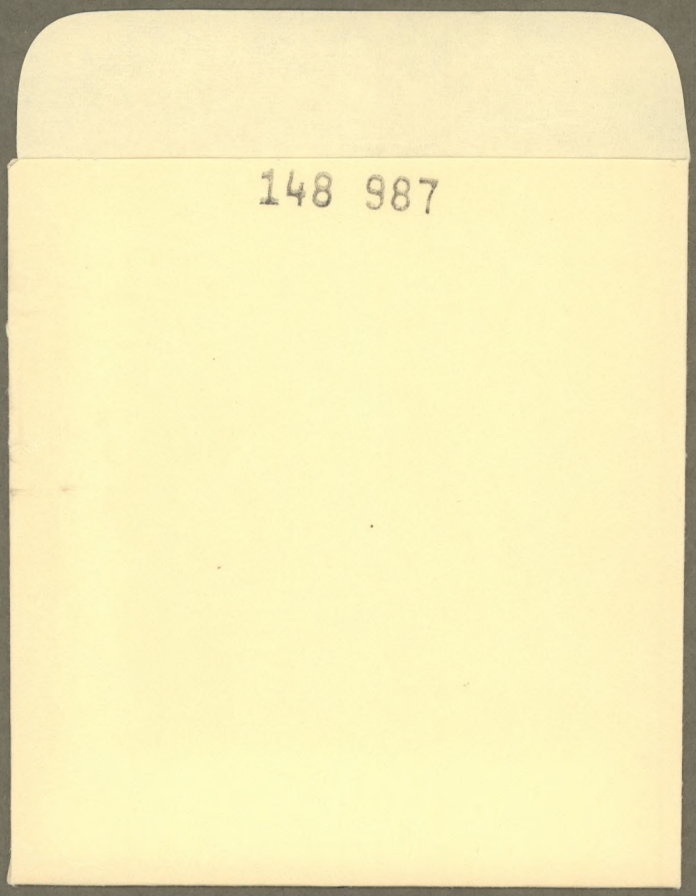

IMPORTANT NOTICE

Technical Memoranda are used to insure prompt dissemination of special studies which, though of interest to the scientific community, may not be ready for formal publication. Since these papers may later be published in a modified form to include more recent information or research results, abstracting, citing, or reproducing this paper in the open literature is not encouraged. Contact the author for additional information on the subject matter discussed in this Memorandum.

U.S. DEPARTMENT OF COMMERCE
Environmental Science Services Administration
Research Laboratories

ESSA Technical Memorandum ERLTM-ARL 11

RESULTS OF VERTICAL-VELOCITY FLUCTUATION MEASUREMENTS IN THE ATMOSPHERIC BOUNDARY LAYER OVER A SALT-HAY MARSH

G.A. Herbert

R.R. Soller(1)

(1) Present affiliation, Air Resources Cincinnati Laboratory, Indiana, Pennsylvania

AIR RESOURCES ENVIRONMENTAL LABORATORY
SILVER SPRING, MARYLAND
February 1969

TABLE OF CONTENTS

RESULTS OF VERTICAL-VELOCITY FLUCTUATION MEASUREMENTS IN THE ATMOSPHERIC BOUNDARY LAYER OVER A SALT-HAY MARSH

G. A. Herbert

and

R. R. Soller

In conjunction with a continuing study of internal boundary layer structure above uniform marsh-grass surfaces, a set of vertical-velocity measurements were made with an ultrasonic anemometer for comparison with the vertical-propeller anemometer, which was part of the principal momentum flux-measuring system in use at a site on the New Jersey shore of the Delaware Bay. The variation in turbulence statistics near the roughness discontinuity was also studied. All records were made within the first 10 m above a salt marsh. Sensitive cup anemometers were used to measure the mean wind profiles in the vicinity of the cut-grass discontinuity. Amplitude statistics, including the skewness and kurtosis, and spectral estimates were computed from all ultrasonic anemometer records. On the assumption of the Kolmogorov form of the spectrum at high frequencies, the dissipation of turbulent kinetic energy was calculated. Comparisons of analog records from propeller anemometer and filtered ultrasonic anemometer records defined the response characteristics of the former instrument.

1.0 INTRODUCTION

A cooperative data-gathering expedition was conducted during the first 2 weeks of October 1966 to compare the Thornthwaite vertical-propeller anemometer with an ultrasonic anemometer. The comparisons were made on a uniform salt-water marsh at the request of Professors Blackadar and Panofsky of the Pennsylvania State University, who were conducting a study of internal boundary layers at this location (see Blackadar et al., 1967). Personnel from the C. W. Thornthwaite Associates

of New Jersey maintained the roughness discontinuity, and operated the vertical-propeller anemometer and the wind and temperature profile instrumentation. We operated the dual ultrasonic anemometer.

2.0 DATA ACQUISITION AND PROCESSING

2.1 Site

The northeast shore of the Delaware Bay contains many large salt-hay marshes. The particular area where the tests were conducted is in Lawrence Township, about 7 mi south-southwest of Bridgeton, New Jersey. The height variation of the marsh was less than 1/2 m, and local relief in the test area was on the order of a few centimeters. A grass area of approximately 5000 m^2 was cut to a height of between 4 to 5 cm to produce a roughness discontinuity with the taller marsh grasses (see fig. 1). The uncut grasses surrounding this area consisted of salt-marsh grasses, sedges, and reeds from 20 to 30 cm tall. The only structure on the marsh was the instrumentation trailer, which was located about 200 m northeast of the cut area. The trees boarding the marsh to the south were almost 1 km from the test area (fig. 2a).

2.2 Instrumentation

The dual ultrasonic anemometer (UA 2/3) used in this study was constructed in 1964 at the Weather Bureau's Observational Test and Development Center, Sterling, Virginia. The original design followed closely the specifications for a "simplified" continuous-wave ultrasonic anemometer suggested by Kaimal (1963). Subsequent field experience led to a number of changes, most important of which was the transistorizing of the preamplifiers to reduce input signal noise and the addition of phase-shifting

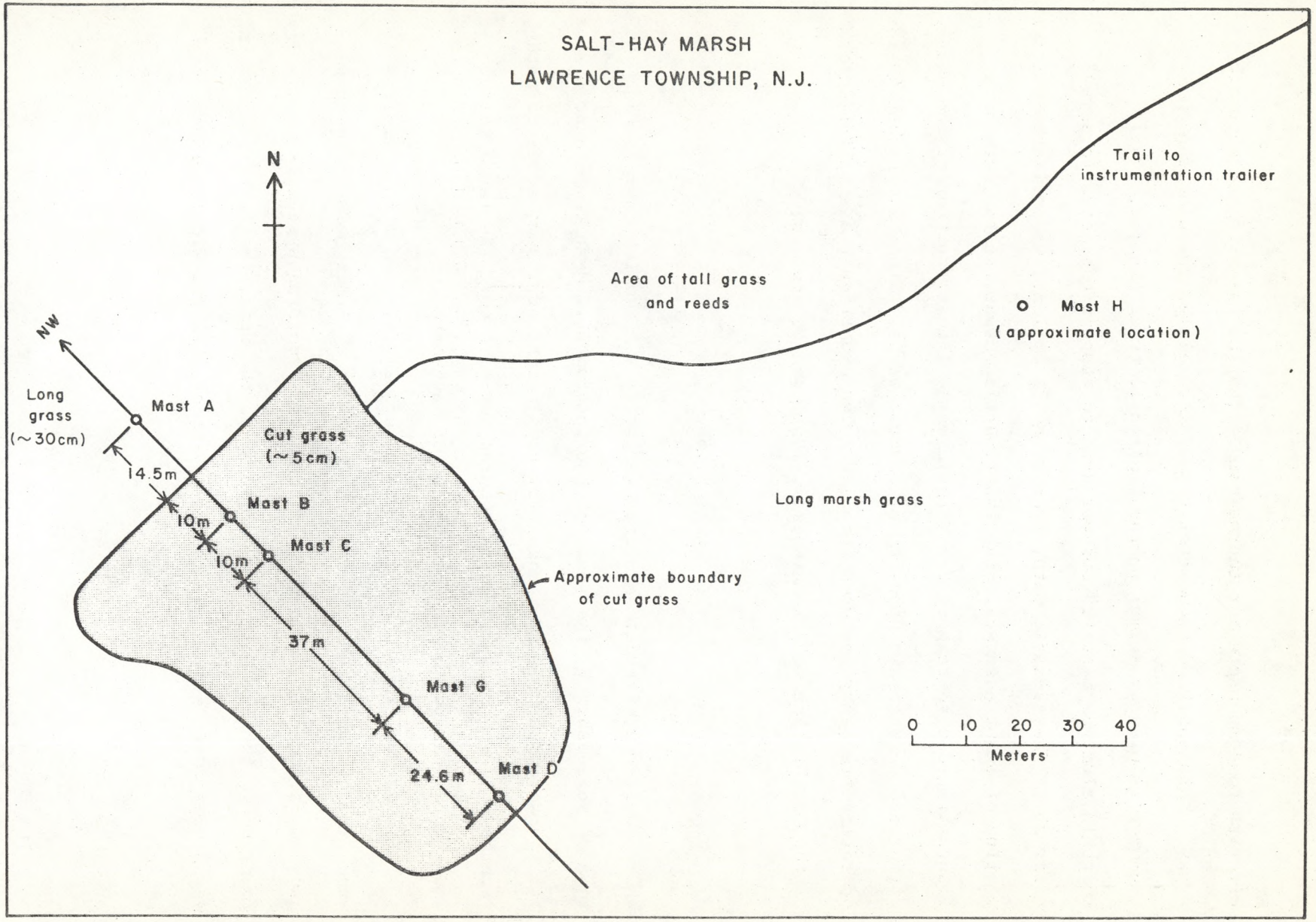

Figure 1. Plan view of the cut grass and surrounding marsh area.

circuits to compensate for thermal and mechanical skew in the acoustic array. This modified anemometer (UA 2/3) resembles the ultrasonic anemometers used by Kaimal on the Cedar Hill tower (Kaimal, 1966). A portable aluminum mast (2" OD) was used to support the acoustic array (fig. 2b). The acoustic path, from 22 to 31 cm long, was oriented vertically to line-of-sight accuracy. The instrument's output, in the form of a fluctuating d-c voltage ($\pm$ 2-V range), was a linear function of the phase difference between two opposing ultrasonic waves. Since a constant 40-kHz operating frequency was used throughout the experiment, a simplified form of the calibration equation (Kaimal, 1963) can be applied,

$$\Delta w = 50.64 \frac{\overline{T}}{d} , \qquad (1)$$

where Δw is the vertical velocity change (cm s^{-1}), which corresponds to a 2π phase shift - the range of the instrument. Mean temperatures ($\overline{T}$, ^{o}K) were measured near the array at a height of 1.5 m; acoustic path lengths (d) were measured to an accuracy of $\pm$ .1 cm. The range voltage was recorded at the beginning and end of each data run.

The output signal from the anemometer was filtered with a single-stage lag circuit (3-dB attenuation at 70 Hz) to limit noise between 60 and 300 Hz, the high frequency limit of the recording system (see fig. 3). To preserve the low frequency component of the data, the filtered signals were recorded in analog FM mode by a 4-track (1/2 in. wide) magnetic tape recorder.

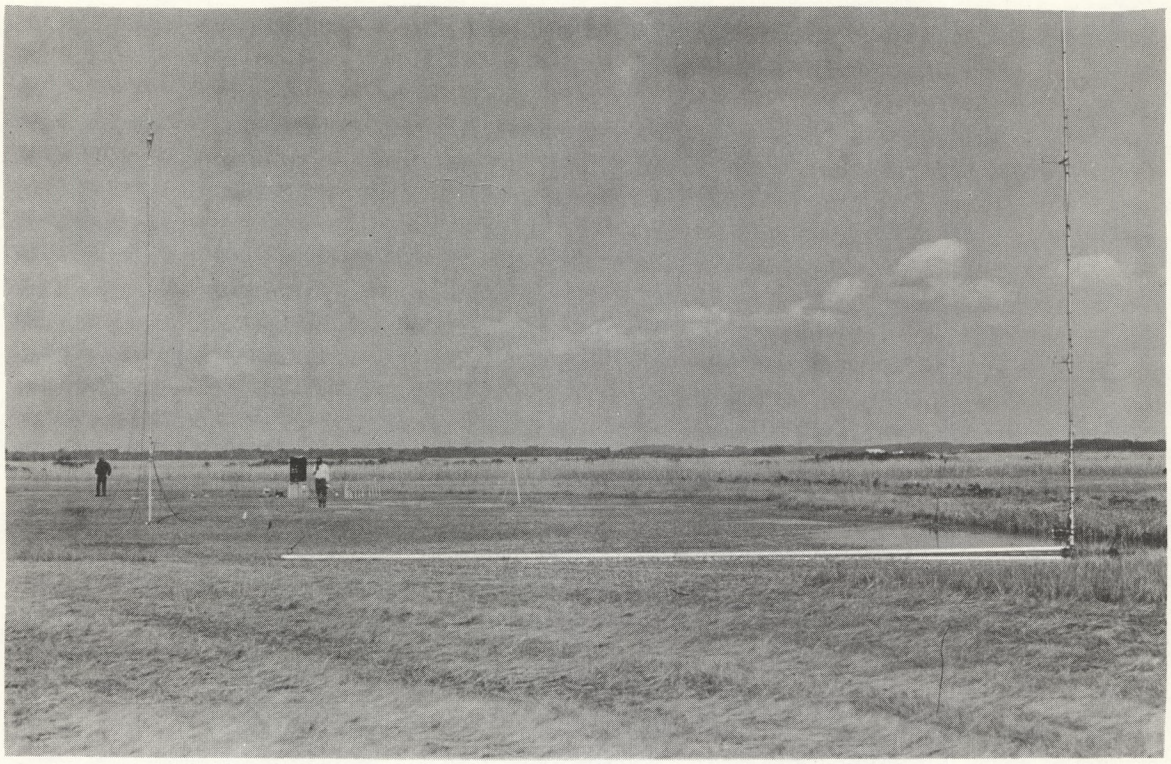

Figure 2 a. Photograph of Thornthwaite vertical-propeller anemometer and UA-2 comparison setup on mast H.

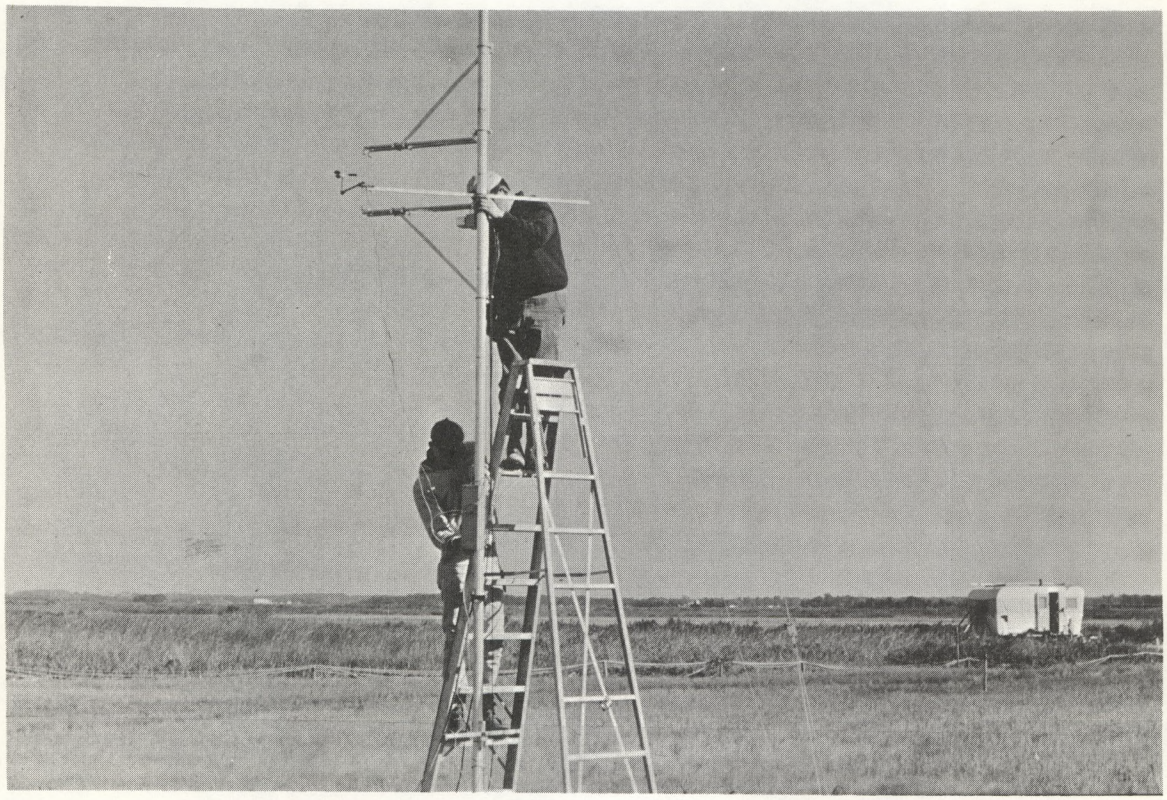

Figure 2 b. Photograph of the marsh site in the cut grass area.

B- 79983

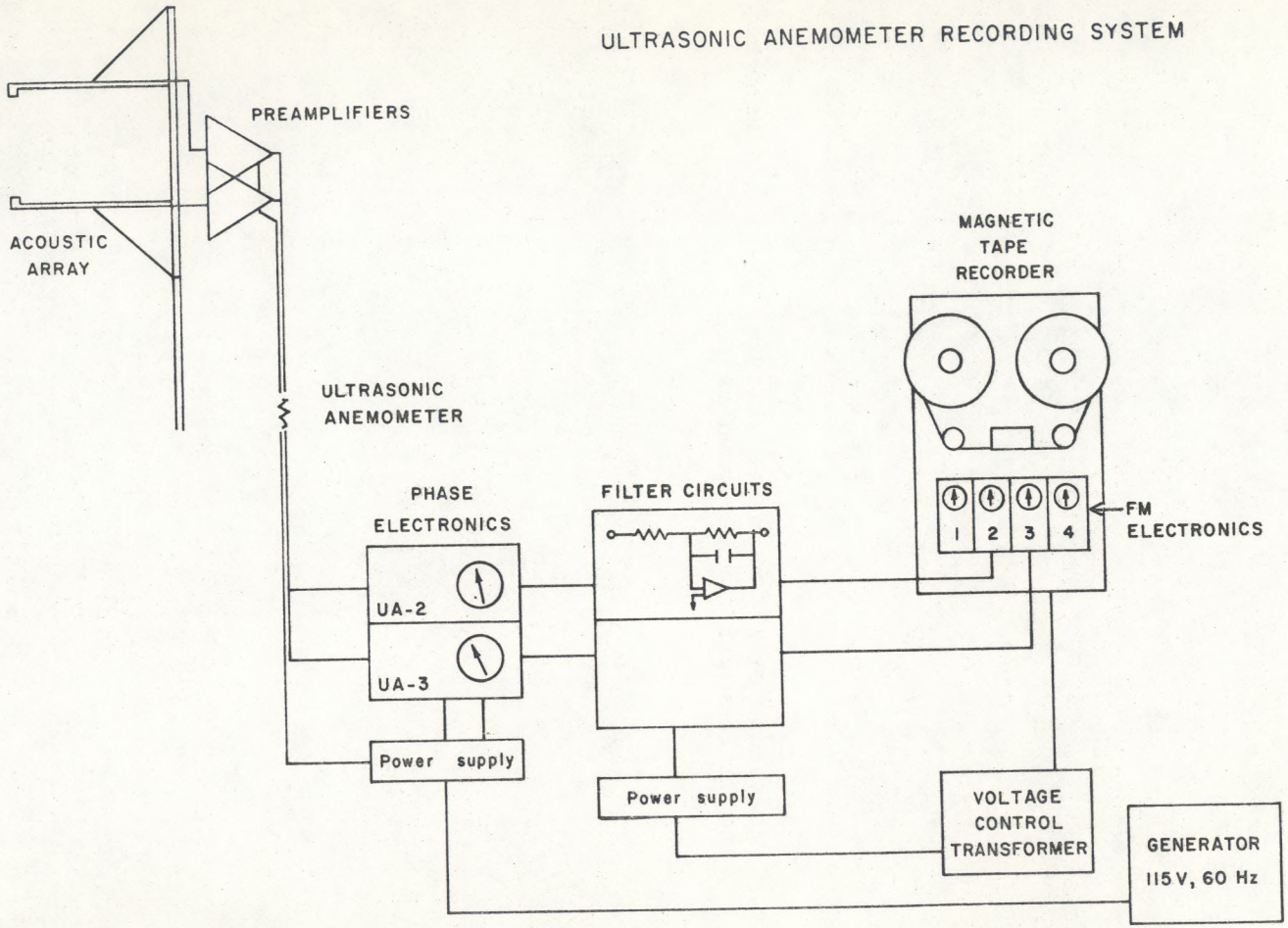

Figure 3. Diagrammatic representation of the measurement system.

All 110-V power requirements were supplied by a 1.5-kW portable generator. A fixed potential was recorded so that drift in the recording system caused by generator speed fluctuations could be evaluated. When observed, the drift was assumed to be common to all channels and was removed from the data, the variations in the reference channel being used as an error signal. Power going to the filter circuits and the tape recorder was regulated by a voltage control transformer.

The propeller anemometer used for comparison with the ultrasonic anemometer was a three-bladed element with a diameter of 15 cm (Thornthwaite et al., 1961). During the first test period, October 6-7, 1966, we were unable to record the propeller system directly because the tape recorder amplifiers were not sufficiently sensitive. For the second test period,October 12-14, 1966, we supplied an amplifier to boost the output voltage to the desired level. After the tests had been completed we learned that this amplifer had a long response time (63 percent of a step function) of approximately 2.5 s for the output impedance of the propeller anemometer (500 ohms). For this reason, the analog magnetic tape records proved to be of little use. A high resolution strip-chart recording of both anemometers, made at the time of the comparisons, was the only valid record from which the two vertical-component measuring instruments could be compared. This comparison is presented in section 5 of this report.

Mean wind speed profiles were measured with cup anemometers at four locations on the marsh (fig. 1); a maximum of seven levels were used: .4, .8, 1.6, 3.2, 6.4, 12.8, and 25.6 m. In general, 10-min averages

were tabulated. Temperatures were measured with mercury-in-glass thermometers at heights of 0.5 and 1.5 m. Run identification numbers, locations, and mean atmospheric conditions are presented in table 1. Averaged wind-speed measurements from 0.4 and 1.6 m levels were used, together with the temperature measurements, to estimate the Richardson number,

$$R_i = \frac{g}{\theta} \frac{\partial\theta/\partial z}{(\partial U/\partial z)^2} \qquad (2)$$

where θ, the potential temperature, was assumed to be adequately represented by the measured air temperature, g is the acceleration due to gravity, and U is the mean wind speed as measured by a cup anemometer. Values so computed are assumed to apply at about the 1-m height.

2.3 Data Processing

All rapid-response measurements were recorded at a tape speed of 7.5 ips and digitized at 1 7/8 ips, with a resulting 4-to-1 data slowdown. The digitizer that transferred the data from analog magnetic tape to an incremental digital (binary) tape operates on four channels of data simultaneously at a rate of four observations per second. (See Priestley (1965) for details concerning this equipment.) Because of the 4X tape slowdown, the true sampling frequency was 16 observations per second. The digital data tapes were "unpacked" from binary to decimal form on a CDC-6600 computer. A listing of the voltage range values in conjunction with (1) yielded data calibration factors for each individual run. A high resolution strip-chart record was also made for each run to

Table 1. Data Log

Date October 1966	Start Time EDT	Duration min	Wind Profile Masts 1.	Test Instrument	Mast[1] Location	Height m	Mean[2] Wind Speed ms^{-1}	Wind Direction deg	Temperature (1.5 m) ^{o}K	Sky	-Ri (1 m)	Run Number
7	1035	10	ABD	UA-2	H	4.0	4.2	270	289	Clear	.013	50A
				PROP	H	4.0						
7	1045	10	ABD	UA-2	H	4.0	4.2	270	289	Clear	.013	50B
				PROP	H	4.0						
7	1325	10	ABCD	UA-2	H	2.0	2.6	180	291	Clear	.066	52
				PROP	H	2.0						
7	1415	10	ABCD	UA-2	H	1.0	2.0	200	291	Clear	MISG	54
				PROP	H	1.0						
12	1318	10	ABCD	UA-2	H	1.0	4.9	280	293	Clear	(.01)	56
				PROP	H	1.0						
12	1440	10	BCD	UA-2	H	2.5	4.8	270	292	Clear	.021	58A
				PROP	H	2.5						
12	1514	10	ABCD	UA-2	H	4.0	5.3	240	292	Clear	.007	58B
				PROP	H	4.0						
12	1555	10	ABCD	UA-2	H	8.0	4.8	270	291	Clear	.005	58C
				PROP	H	8.0						
13	1330	12	AB	UA-2	A	1.6	2.9	140	293	/-0	-	60A-2
				UA-3	B	1.6	3.0					60A-3
13	1342	12	AB	UA-2	A	1.6	2.9	140	293	/-0	-	60B-2
				UA-3	B	1.6	3.0					60B-3
14	1020	15	None	UA-2	G	9.8	MISG	160	293	Clear	-	62-2
				UA-3	G	1.0	MISG					62-3

[1] Shown in figure 1.

[2] Cup-anemometer wind speeds from the mast closest to the test mast were used. Means were for the duration of the run at test instrument height.

Table 1 (Continued)

Date October 1966	Start Time EDT	Duration min	Wind Profile Masts 1.	Test Instrument	Mast[1] Location	Height m	Mean[2] Wind Speed ms^{-1}	Wind Direction deg	Temperature (1.5 m) ^{o}K	Sky	-Ri (1 m)	Run Number
14	1050	15	None	UA-2	G	9.8	MISG			Clear	-	64-2
				UA-3	G	2.0	(5.2)	160	293			64-3
14	1315	15	ABC	UA-2	G	9.8	5.6			Cu w	-	66-2
				UA-3	G	3.0	5.0	150	294	/-◐		66-3
14	1405	15	ABC	UA-2	G	4.0	5.8			/-⊕	-	68-2
				UA-3	G	1.0	5.3	130	293			68-3
14	1450	15	ABCD	UA-2	G	2.0	5.6	150	293	/-⊕	-	70-2
				UA-3	G	2.0	5.6					70-3

evaluate the steadiness and general noise quality of the recording. A sample of these traces is presented in section 5. In two cases it was necessary to break the run into two units: in run 50 a slow drift was observed in the latter half of the run, and excessive noise appeared late in run 60.

After the data had been calibrated, the mean vertical velocity was calculated in the usual way and removed from the time series w(t), which was assumed to be stationary:

$$w'(t) = w(t) - \bar{w}. \tag{3}$$

In most cases the mean value was below the accuracy limits of the instrument, a value of about $\pm$ 8 cm s^{-1}. Higher statistical moments were calculated directly from the vertical-velocity fluctuation values, w'(t), the variance,

$$\sigma^2 = \overline{(w'(t))^2}, \tag{4}$$

the skewness,

$$S_k = \overline{(w'(t))^3}/\sigma^3, \tag{5}$$

and the kurtosis,

$$K = \overline{(w'(t))^4}/\sigma^4, \tag{6}$$

where normally distributed data have a skewness of zero and a kurtosis of 3. In all cases, the overbar indicates a time average for the full run. A discussion of these amplitude statistics is contained in section 3.

Spectral density estimates were calculated from the resolution frequency of 10^{-2} Hz to the Nyquist frequency of 8 Hz. These estimates were obtained from the cosine transform of the smoothed autocorrelation function, the method suggested by Blackman and Tukey (1958, p. 33). The autocorrelation $C(\tau)$ is formulated by normalizing the autocovariance $R(\tau) = \overline{w'(t)w'(t+\tau)}$ by the variance $\overline{(w')^2}$,

$$C(\tau) = R(\tau)/\overline{(w')^2} \quad , \tag{7}$$

where τ is the time lag between data points. Autocorrelations values were assumed to be "well-behaved" (positive definite and continuous), a requirement for computing spectral density estimates. In this analysis a hamming-type lag window,

$$\begin{aligned} D(\tau) &= 0.54 + 0.46 \cos \frac{\pi\tau}{Tm} \qquad \tau < Tm \\ &= 0 \qquad\qquad\qquad\qquad \tau > Tm \end{aligned} \quad , \tag{8}$$

with a period of Tm was used to smooth the autocorrelation function $C(\tau)$,

$$C^*(\tau) = C(\tau) \quad (D(\tau)), \tag{9}$$

before transforming the data. When the smoothed autocorrelation values are written in terms of lag numbers r, where $r = \tau/\Delta t$, and Δt is the data interval, the normalized spectral density function is

$$S(n) = \Delta t \left[C^*(0) + 2 \sum_{k=1}^{M-1} C^*(r) \cos \frac{\pi rk}{M} + C^*(M) \cos(\pi k) \right] \quad 0 \leq k \leq M, \tag{10}$$

where frequency $n = k/2\Delta tM$. Lag M values of 800, 320, 160, 80, and 16 were used in this analysis.

The digitizing equipment summed the frequency content of the analog tape records for 1/16-s intervals, which amounts to a "box-car" type averaging of the original data. Blackman and Tukey (1958, p. 95) discuss the transform pair relating to this data window and show the spectral window to be

$$Q_o/\Delta t = \frac{\sin n\,\Delta t/2}{n\,\Delta t/2} . \qquad (11)$$

The data transfer function, $(Q_o/\Delta t)^2$, is given by Pasquill (1962, fig. 1.5). All spectra were corrected with this function without accounting for aliasing. The amount of aliasing observed in the computed spectra was small, and when excess energy was observed it was confined to the octave bounded on the upper end by the Nyquist frequency. The combination of decreasing spectrum in the frequency band 8 Hz to 16 Hz and beyond, data filtering as shown in (11), and spacial averaging by the acoustic array with a transmission of about 0.4 at the Nyquist frequency ($U = 4\ ms^{-1}$) (Mitsuta, 1966) limits the amount of energy available for aliasing. The resulting "well-tapered" spectra are discussed in subsequent sections.

3.0 RESULTS OF ULTRASONIC ANEMOMETER MEASUREMENTS

3.1 Amplitude Statistics

Values of the first four moments were calculated for each complete ultrasonic anemometer run, and from these calculations the standard deviation, skewness, and kurtosis values (table 2) were computed. Mean

values were not tabulated, because they were insignificant in comparison with the resolution limits set by the uncertainty in the acoustic array alignment and by the electronic drift in the anemometer, filter circuits, and recorder system. Measured standard deviations of the vertical wind component, σ , were found to be relatively insensitive to changes in height but strongly influenced by wind speed, so that in the mean $\sigma/\bar{U} = 0.088$, which agrees well with the 0.090 computed from Brookhaven tower data (Deacon, 1959). The small positive skewness values measured in this experiment are consistent with findings of Gurvich (1960) and Maitani and Mitusta (1967). The negative skewness values reported from data collected on October 7, 1966, are suspect because of a basic uncertainty in the polarity of the calibration. An examination of the strip-chart record of the UA-3 data collected at 1405 EDT, October 14, 1966, clearly indicated a number of large intermittent spikes to be the cause of the large negative skew. Such spikes resemble the noise associated with analog-tape imperfections or "dropouts." The kurtosis, or flatness, factors, adjusted by the value for normally distributed data, are, with only one exception, small positive values (see table 2).

In a study of winds over open water surfaces, Pond and Stewart (1965) found small kurtosis values when considering the full frequency band represented by the data. After filtering the low frequencies out of the record, they observed a much larger ($k = 17$) value. To examine the amplitude statistics in the high frequency region of these data, we applied a digital filter centered at 1.42 Hz ($\pm$ 0.42 Hz), as shown in figure 5, to the data. The standard deviation of the filtered data (table 2) was reduced by more than a factor of 2, while in most cases the skewness was a factor of

Table 2. Results of Ultrasonic Anemometer Measurements

Date	Starting Time	Instrument	Complete Run			Filtered Run			Complete Runs				
			σ ms^{-1}	S_k	k-3	σ ms^{-1}	S_k	k-3	Low Frequency -5/3 Hz	ε $10^{-4} m^2 s^{-3}$	u_* $(.4\ z\varepsilon)^{1/3}$ ms^{-1}	u_* $.77\ \sigma$ ms^{-1}	u_* $.4\ z\ \frac{\partial \bar{u}}{\partial z}$ ms^{-1}
7 Oct	1035	UA-2	.33	-.34	1.05	.10	-.03	1.46	0.8	79	.24	.26	.36
	1045	UA-2	.40	-.47	.54	.11	-.02	1.72	0.6	150	.29	.31	
	1325	UA-2	.27	-.16	1.37	.08	-.01	1.61	No	(77)	(.18)	.21	.25
	1415	UA-2	.20	.09	.26	.08	.02	2.17	1.5	78	.15	.15	.17
12 Oct	1318	UA-2	.49	.02	- .003	--	--	--	No	(1500)	(.40)	.38	.54
	1440	UA-2	.48	.23	.14	.17	-.01	+ .82	1.5	590	.39	.37	.35
	1514	UA-2	.44	.28	.56	.18	.01	1.70	1.0	370	.39	.34	.47
	1555	UA-2	.65	.10	.30	.18	.03	1.95	1.5	110	.33	.50	.32
13 Oct	1330	UA-2	.20	.35	.47	.08	.03	1.22	4.0	40	.14	.15	.24
	1330	UA-3	.22	.01	.54	.08	.01	1.59	No	(66)	(.16)	.17	.14
	1340	UA-2	.26	.35	.81	.07	.01	1.53	No	(49)	(.15)	.20	.24
	1340	UA-3	.20	.01	.65	.07	.04	0.94	2.0	52	.15	.15	.14
14 Oct	1020	UA-2	.35	-.34	.13	.09	.02	1.52	No	(30)	(.23)	.27	MISG.
	1020	UA-3	.25	-.01	.33	.10	.02	.67	No	(140)	(.18)	.19	"
	1050	UA-2	.38	.15	.47	.09	.01	2.60	0.8	42	.26	.29	"
	1050	UA-3	.32	.16	.34	.12	.02	1.46	2.0	160	.23	.25	"
	1315	UA-2	.41	.22	.05	.10	.04	1.50	No	63	.29	.32	"
	1315	UA-3	.36	.17	.57	.12	.05	1.80	1.5	140	.26	.28	"
	1405	UA-2	.36	.18	.37	.11	.03	.98	1.0	180	.26	.28	"
	1405	UA-3	.37	-1.07	4.18	.13	-.03	2.10	No	--	---	.29	"
	1450	UA-2	.38	.15	.35	.14	.02	2.10	1.0	250	.27	.29	"
	1450	UA-3	.36	.18	.99	.14	.02	1.04	No	260	.28	.28	"

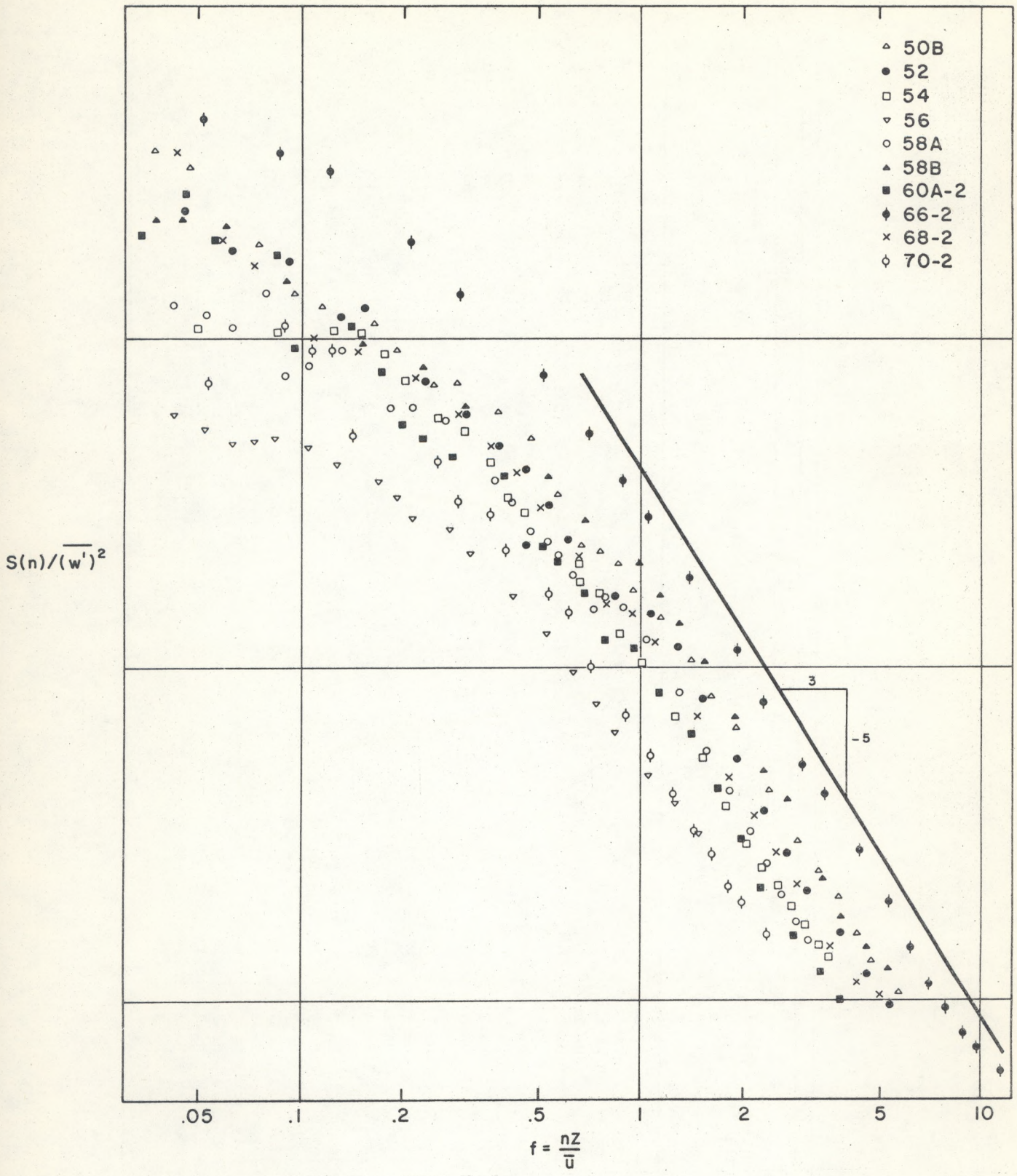

Figure 4. Normalized spectral density estimates vs. nondimensional frequency of UA-2 data. The normalized spectral estimates are in units of Hz^{-1}.

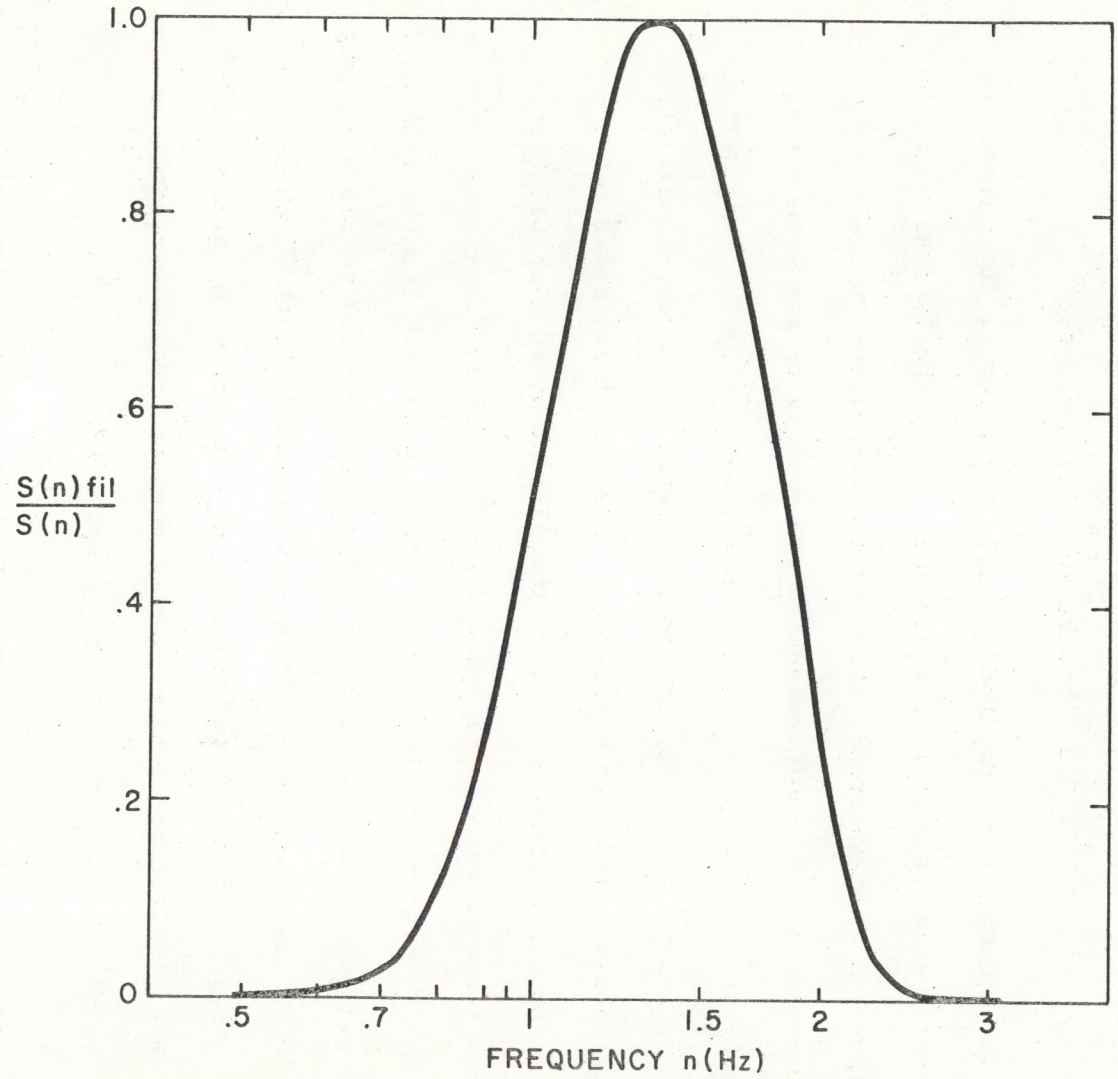

Figure 5. The symmetrical digital filter (49 points) used to band-pass filter data reported in table 2.

10 smaller. On the other hand, the kurtosis increased by factor of 2 or more, which is consistent but smaller than the values reported by Pond and Stewart (1965) and Gurvich (1966) for much higher frequency bands.

3.2 Spectral Density Estimates

The spectra were computed for all UA-2 records, but only those records that correspond to a profile measurement of the horizontal wind speed appear in figure 6. The spectral estimates are normalized by the variance, and the frequency scale is nondimensionalized according to the method suggested by Panofsky and McCormick (1960), $f = nz/U$, where U is the mean horizontal wind speed as measured by a cup anemometer. This frequency normalization significantly reduces the difference in spectral estimates between runs. Most of the spectra that do not follow the -5/3 slope at high frequencies are from records measured at heights below 2 m. This is to be expected because of path-wise averaging by the acoustic array, with path lengths ranging from .22 to .31 m, yielding a "distance constant" from .27 to .38 m, a large portion of instrument height. The low frequency limit of the -5/3 slope seems to be about $f = 1$, which is twice as large as the value predicted by MacCready (1962). Spectral estimates computed from all recordings made during this experiment are contained in the appendix.

3.3 Dissipation of Turbulent Kinetic Energy

By virtue of the atmosphere's large Reynolds number, Kolmogorov (1941) hypothesized a region, at large wave numbers, where turbulent fluctuations are both locally isotropic and insensitive to viscous forces, the inertial

subrange. In this region the three-dimensional energy spectrum (E(k)) takes the form given by Lumley and Panofsky (1964),

$$E(k) = \alpha \varepsilon^{2/3} k^{-5/3} , \tag{12}$$

where ε is the rate of energy dissipation, and k is the wave number. It is immediately apparent that measuring the spectra at a single wave number is all that is necessary to define the entire subrange. A formulation relating the longitudinal one-dimensional spectrum ($F_{long}(k)$) to the three-dimensional spectrum in isotropic turbulence (Lumley and Panofsky, 1964, p. 30) is

$$E(k) = k^3 \frac{\partial}{\partial k} \left[\frac{1}{k} \frac{\partial F_{long(k)}}{\partial k} \right],$$

where

$$\frac{1}{2} (u')^2 = \int_0^\infty F_{long}(k),$$

u' representing the fluctuations in the mean-wind direction as defined in (3) of the vertical wind component.

In terms of the longitudinal one-dimensional spectrum we obtain

$$F_{long}(k) = \alpha_{long} \varepsilon^{2/3} k^{-5/3} , \tag{13}$$

where $\alpha_{long} = 9/55\, \alpha$. To obtain the desired results for the lateral one-

dimensional spectrum ($F_{lat.}(k)$), we can apply the spectral form of the von Kármán-Howarth equation (Batchelor, 1953, p. 50),

$$F_{lat.}(k) = 1/2 \left[F_{long.}(k) - k \frac{\partial}{\partial k} F_{long.}(k) \right] ,$$

to (13). We then obtain

$$F_{lat.}(k) = 12/55\ \alpha\ \varepsilon^{2/3}\ k^{-5/3} . \qquad (14)$$

All measurements are collected in a fixed-point-time framework and thus (14) must be transformed from wave-number space [radians cm^{-1}] into frequency space [Hz]. We do so by employing Taylor's hypothesis, which assumes that the turbulent part of the flow is being transported by the mean wind as if it were "frozen." This hypothesis is written in the form $k = 2\pi n/U$. At the same time, the spectrum S(n) as determined in (10) can be defined as

$$\int_0^\infty S(n)\ dn = \overline{(w')^2} , \qquad (15)$$

and (14) can be rewritten

$$S(n) = 24/55\ \alpha\ (2\pi)^{-2/3}\ U^{2/3}\ \varepsilon^{2/3}\ n^{-5/3} . \qquad (16)$$

If we assume that the observed -5/3 slope is a low-frequency extension of the spectrum predicted for the inertial subrange, we can obtain estimates of the rate of turbulent energy dissipation from a single spectral estimate.

Solving (16) for ε yields

$$\varepsilon = A \frac{S(n)^{3/2} n^{5/2}}{U}, \qquad (17)$$

where

$$A = \frac{2\pi}{(24/55\ \alpha)^{3/2}}.$$

The universal constant α has been determined in a wind tunnel by Gibson (1963) and Kistler and Vrebalovich (1966) and in the atmosphere by Pond et al. (1966). A mean value of $\alpha = 1.47$ seems to agree with the largest number of these observations.

Before discussing the dissipation estimates, let us examine the two main assumptions used for deriving (17). It is clear from the analysis by Pond et al. (1963) that the small scales at which isotropic turbulence would be expected ($kz \gg 4.5$) are only defined at the highest frequencies at the highest 8- and 9.8-m working levels. Normally the octave bounded by the Nyquist frequency is also partly contaminated by aliased energy from higher frequencies. We therefore have to assume that the observed -5/3 spectral slope is uniform low-frequency extensions of the spectral shape at higher frequencies in the Kolmogorov region. With regard to the second assumption, Pond et al. (1966) state the low wave number bound to the region over which Taylor's hypothesis can be applied as $kz \gg 1$. In our experiment at 3.5 Hz, the frequency at which ε values will be computed, the restriction is satisfied at heights of 2 m and above if we assume $U = 5\ ms^{-1}$.

Estimates of the energy dissipation ε were computed for all runs independently of an observed -5/3 spectral slope (see table 2). In two cases of uniform height, runs 54 and 56 and 50 and 68-1, ε values increase with increasing wind speed. With wind speed relatively constant, runs 58A to 58C show a consistent decrease in ε with increasing height (590 $cm^2\ s^{-3}$ at 2.5 m and 110 $cm^2\ s^{-3}$ at 8 m). In another comparison, runs 66-2 and 70-2 ($u = 5.6\ ms^{-1}$), the dissipation at 9.8 m was estimated to be 63 $cm^2\ s^{-3}$, while at 2 m it was 260 $cm^2\ s^{-3}$.

3.4 Friction Velocity Estimates

If we consider the budget of turbulent kinetic energy in horizontally homogeneous turbulence in balanced conditions, then (Lumley and Panofsky, 1964),

$$0 = u_*^2 \frac{\partial U}{\partial z} + gH/C_p T - \frac{\partial \overline{ew}}{\partial z} - \frac{\partial\ \overline{wP}/\rho}{\partial z} - \varepsilon \ . \qquad (18)$$

In the surface layer under near-neutral conditions, two important restrictions render a very useful result:

1. The term $\frac{\partial\ wP/\rho_o}{\partial z}$ is small compared with the other terms in the equation and can be neglected (Lumley and Panofsky, 1964).
2. As suggested by observations, the sensible heat flux H is small, and the "buoyancy term" $gH/C_p\rho T$ is balanced by the vertical advection of turbulent kinetic energy $\frac{\partial\ \overline{ew}}{\partial z}$.

The assumption of near-neutral conditions in this instance is a valid one because the availability of surface water and dense vegetation on the marsh

markedly reduced the vertical flux of sensible heat, which, when coupled with steady winds, led to a near-neutral stability regime in the lowest 10 m. The small Richardson numbers observed in clear-sky situations (see table 1) further substantiate this restriction. With these assumptions, (18) is reduced to the form

$$0 = u_*^2 \frac{\partial U}{\partial z} - \varepsilon \ ,$$

which when solved for the friction velocity becomes

$$u_* = \left[\varepsilon \ \frac{\partial U}{\partial z}^{-1} \right]^{1/2} \ , \tag{19}$$

and from this relationship independent estimates of u_* are derived. For neutral conditions, where $z_o \ll z$,

$$\frac{\partial U}{\partial z} = \frac{u_*}{kz} \ ,$$

and rewriting (13) yields

$$u_* = (\varepsilon k z)^{1/3} . \tag{20}$$

For comparison, values of $u_* = kz \frac{\Delta U}{\Delta z}$ are also tabulated for those records during which wind profiles were measured (see table 2).

In a recent paper, Busch and Panofsky (1968) found that for near-neutral conditions, the friction velocity could be estimated by the standard

deviation of the vertical wind component σ:

$$u_* = 0.77\ \sigma\ . \qquad (21)$$

Friction velocities computed in this manner are also listed in table 2. Clearly, the differences between friction velocities computed from (20) and (21) are much smaller than the differences derived from a comparison of (19) and (20) or (19) and (21).

4.0 SIMULTANEOUS MEASUREMENT SETS - UA-2/3

4.1 Direct Instrumental Comparison

At the end of this experiment, the two acoustic anemometers were placed alongside each other so that systematic differences between anemometers could be evaluated and applied to the interpretation of previous measurements at different heights and locations. Both acoustic arrays were adjusted to identical path lengths (.22 m) and placed on 2-m high masts separated by approximately 0.1 m. A 15-min comparison, designated run 70, was begun at 1450 EDT on October 14, 1966. Measured standard deviations of the vertical wind component (σ) were 0.38 ms^{-1} for UA-2 and 0.36 ms^{-1} for UA-3, a difference that is consistent within the limits of calibration accuracy. The normalized spectral densities, $\left[nS(n)/\overline{(w')^2}\right]$, agree well for all frequencies below 1 Hz (fig. 6). The confidence intervals, shown at various frequencies, were determined by assuming a chi-squared distribution with an equivalent number of degrees of freedom (Blackman and Tukey, 1958, p. 22); 90 percent confidence intervals are plotted (fig. 6). Above 3 Hz, the UA-3 system shows significantly greater variance than its neighbor. There is also

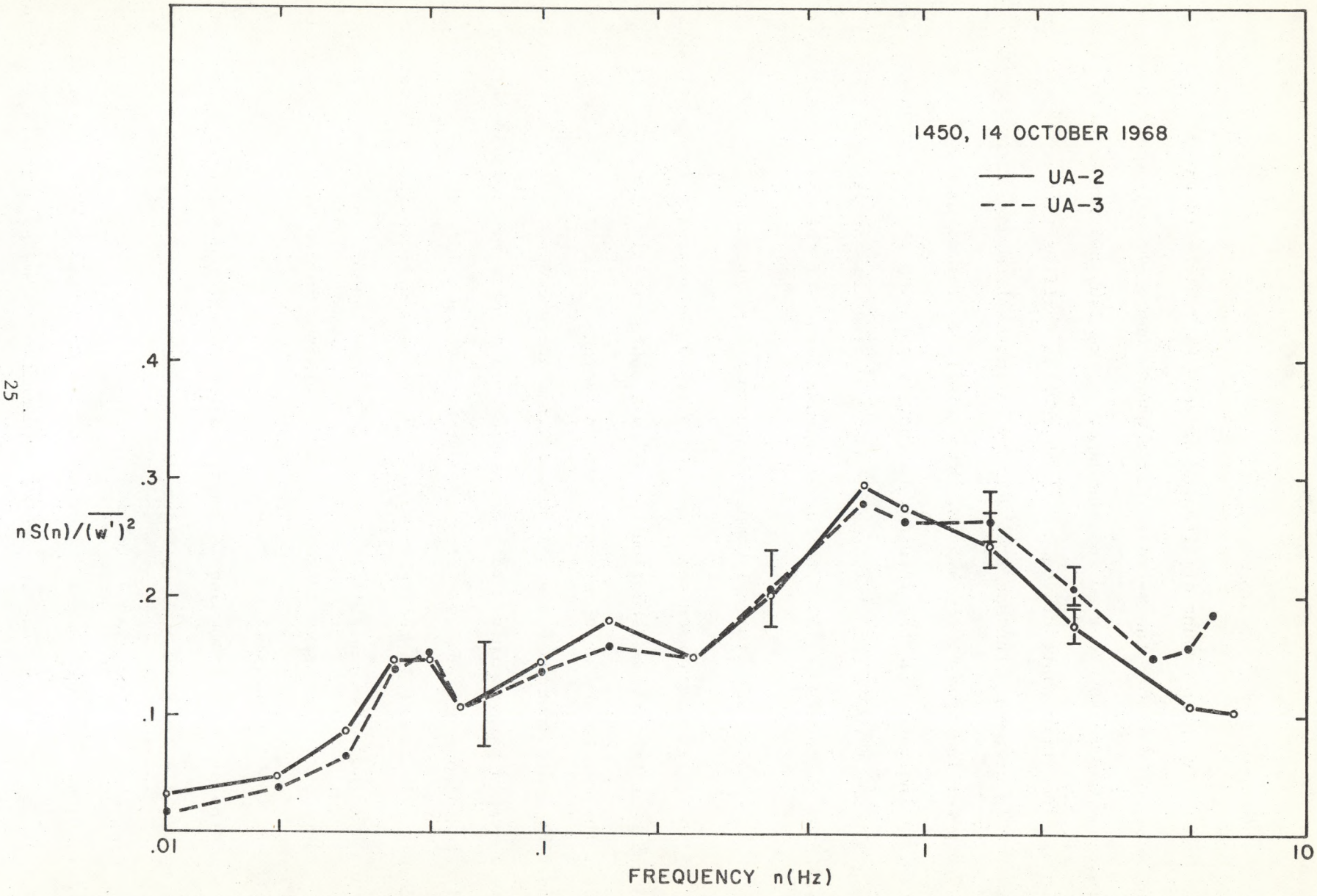

Figure 6. Normalized spectral estimates for 1450 EDT, October 14, 1966 (run 70).

an unusually large amount of aliasing above 4 Hz, which indicates the presence of noise in the 8- to 16-Hz frequency band. In only one other instance was noise observed in this band, on the 1405 EDT run October 14, 1966. The strip-chart playback of both records verifies this noise, but its source is unknown. The spectral density estimates from UA-2, run 70, obey a -5/3 power law from 1.0 to 4.5 Hz. Wind profiles from masts C and D (see fig. 1) indicate that the internal boundary separating the two roughness regimes was between 3 to 4 m high at mast G during this comparison. The fetch of cut grass was 30 m to the southeast corner of the test area.

4.2 Longitudinal Comparison Across Discontinuity

The first comparison was conducted at 1330, October 13, 1966, on masts A and B at the grass discontinuity. With a southeasterly wind, the flow was from the cut to the uncut grasses with an average cut grass fetch of 70 m to mast B. Both instruments were located 1.6 m above ground: UA-2 on mast A, 14.5 m from the cut in the tall grass and UA-3 on mast B. Because of long drift and some extraneous system noise that developed late in the run, a result of a change in generator speed, the run was divided into two parts, runs 60 A and 60 B. A signal from the reference channel was used to remove the drift, but excessive noise above 1 Hz remained in run 60 B and prohibited its use in this analysis.

Wind profiles from masts A and B and the normalized spectral densities for run 60 A are presented in figure 7. The mast A profile shows a deceleration of winds below 2 m as a result of their 14.5-m passage over the tall grass. The wind speed difference at 1.6 m is barely significant at 0.1 ms^{-1}. Similarly, the difference between the estimated standard deviations

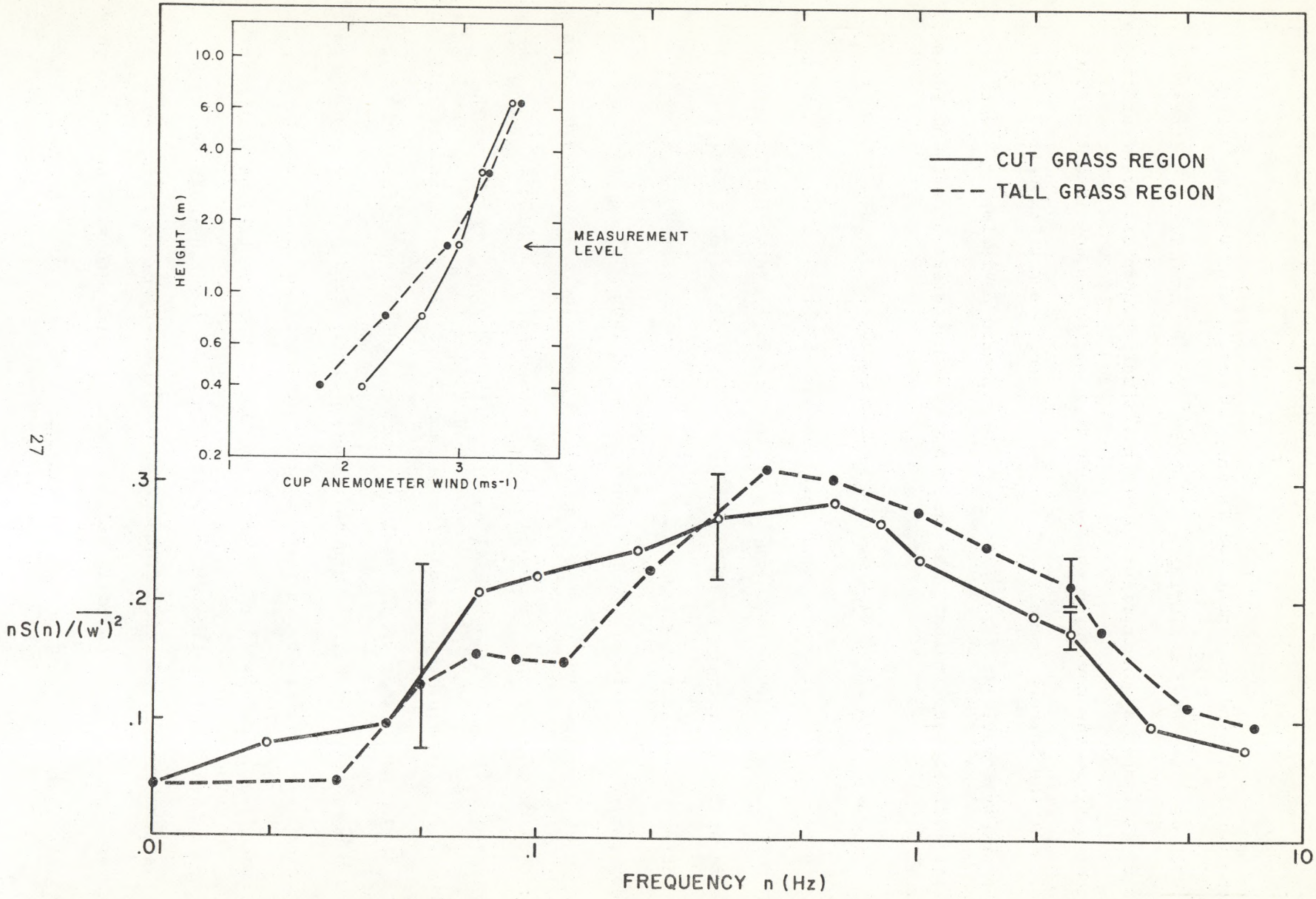

Figure 7. Normalized spectral estimates and wind profiles from mast A and B, run 60 A.

of the vertical wind component (σ) is only 0.02 ms^{-1}, with UA-2 measuring σ = 0.20 ms^{-1} and UA-3 measuring σ = 0.22 ms^{-1}. The normalized spectral density estimates shown in figure 7 are not significantly different at any frequency since the deviation observed above n = 1 Hz is consistent with the results of the "direct comparison" run 70. There does not, therefore, seem to be any systematic difference between the standard deviation or spectral density estimates to indicate the influence of a different underlying surface.

4.3 Vertical Comparison Above Cut Grass

Three of the four comparisons recorded on October 14, 1966 (run 62 at 1020 EDT, run 64 at 1050 EDT, and run 66 at 1315 EDT), are of particular interest because of the uniformity of the 9.8-m level spectral estimates (fig. 8), indicating the relatively steady flow conditions that existed during this midday period. The fourth comparison (run 68 at 1405 EDT) is not usable because of excessive system noise in UA-3. A small increase was observed in the standard deviation of the vertical wind component from 0.35 ms^{-1} in the morning to 0.41 ms at 1315 EDT (table 2). With the wind from the south-southeast, all measurements made at a height of 9.8 m represented the tall grass flow. For direct comparison, simultaneous records were made at 1-, 2-, and 3-m heights (runs 62, 64, and 66 respectively). Wind profile measurements indicated that the 1- and 2-m records are representative of the smooth flow, while the 3-m height is in the transition zone. The spectral estimates for the upper level are relatively constant, but at the lower heights the curves shift systematically to lower frequencies with increasing heights. Both filtered and unfiltered kurtosis values (table 2) increase with height so that it is difficult to determine what, if any, part of the large values at 3 m

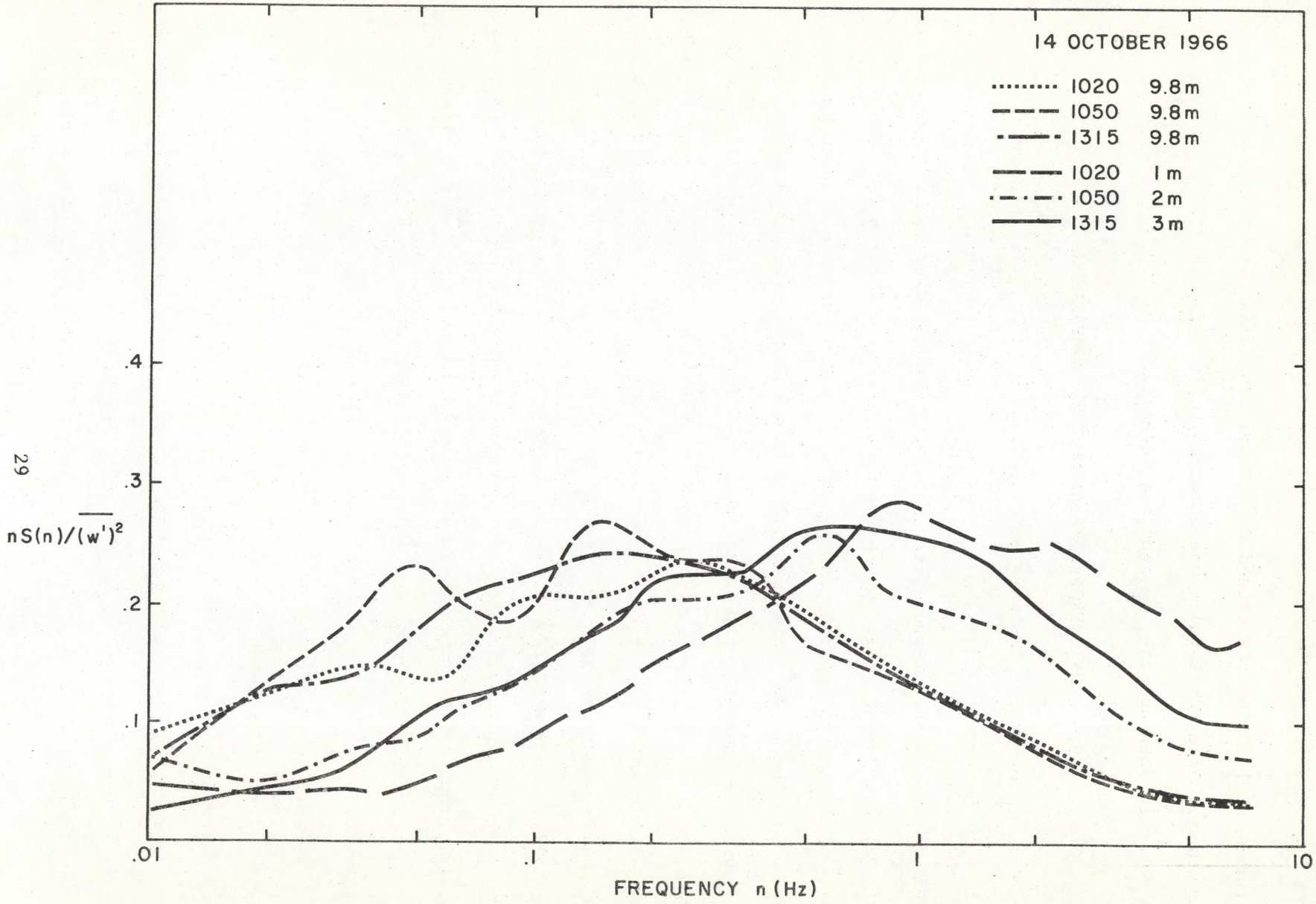

Figure 8. Normalized spectral estimates from runs 62, 64, and 66.

(run 66 at 1315 EDT) is caused by intermittency associated with the internal boundary. A kurtosis value was observed to increase in a similar manner on October 12 data at 2.5-, 4-, and 8-m heights.

5.0 SONIC/PROPELLER ANEMOMETER COMPARISON

Four 10-min records were made on October 12 (run 56 at 1318 EDT, 58 A at 1440, 58 B at 1514, and 58 C at 1555) for direct comparison between the Thornthwaite vertical-propeller anemometer and the ultrasonic anemometer (UA-2). Figure 2b shows the instrumentation mounting, with the control hub of the propeller located opposite the midpoint of the acoustic path and approximately 0.15 m to the left. This configuration was mounted at four heights (1, 2.5, 4, and 8 m) in an attempt to delineate the response characteristics of the two sensors. The change from 4 to 8 m (runs 58 B and 58 C) showed the most noticeable shift in the UA-2 spectrum (fig. 9). While the magnitude of the wind decreased from 5.3 ms^{-1} (run 58 B) to 4.8 ms^{-1} (run 58 C), the standard deviations increased from 0.44 ms^{-1} to 0.65 ms^{-1}. The spectra indicate that the largest contribution to this increase in variance is at lower frequencies. If the propeller anemometer output had been properly recorded on magnetic tape, a transfer function could have been constructed from the spectra of both records.

Because of a sluggish amplifier, which was placed in the propeller anemometer circuit, the data were not usable. An alternative approach, suggested by a study of the original strip-chart records, was to compare portions of the propeller anemometer traces with a low-pass filtered version of the sonic trace. The original, unfiltered, records are shown in figures 10 (run 58 B) and 11 (run 58 C), traces a and b. Four low-pass filters were

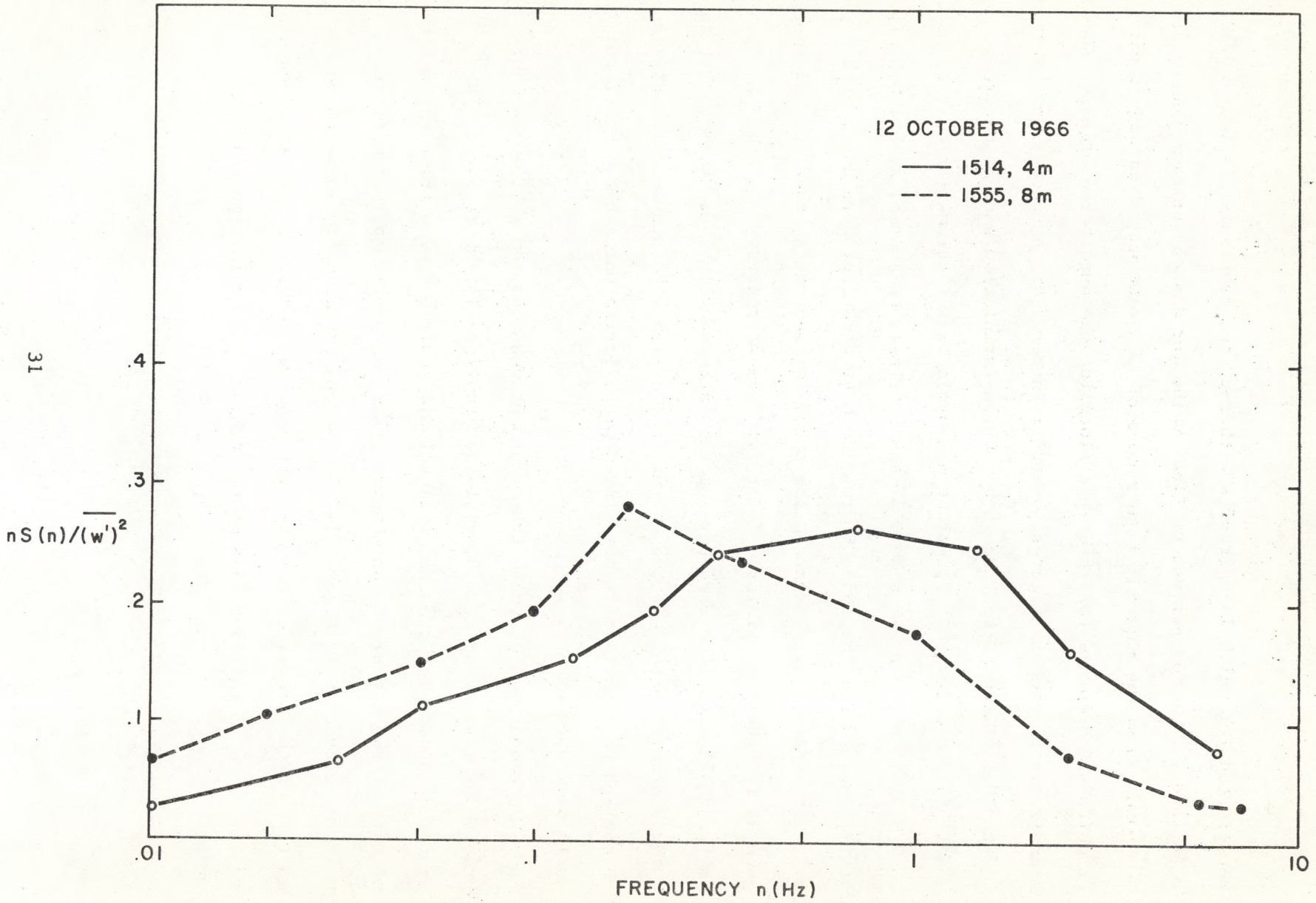

Figure 9. Normalized spectral estimates from runs 58 B and 58 C.

constructed for which lag circuits with r-c time constants τ = 0.16, 0.32, 0.64, and 1.28 s (63 percent of final value for a step function) were used. A voltage from the magnetic tape record of UA-2 was passed through these circuits and recorded for reference alongside the unfiltered signal. These signals are plotted in figures 10 and 11 in terms of the equivalent "distance constant" L of the filter, where $L = U\tau$, a formulation used by MacCready and Jex (1964) to describe first-order meteorological instrumentation response. For the 1514 EDT run (58 B at 4 m) three filters were used, at L = 0.8, 1.7, and 2.5 m, and for the 1555 EDT run (58 C at 8 m) four were used, at L = 0.8, 1.5, 2.3, and 3.1 m. Comparing the propeller records to the filtered sonic records in figure 10 yields a "best fit" somewhere between L = 1.7 and 2.5 m. In figure 11, the fine structure of the large oscillations seems to fit the L = 2.3 m curve best. To the extent that a simple "distance constant" can be applied to a vertically orientated propeller, a value between 1.7 and 2.3 m would seem appropriate.

The comparison of these traces and others measured at lower heights (run 56 at 1 m and 58 at 2.5 m) yielded two interesting results. The propeller anemometer does not follow small amplitude, low frequency deflections as well as the ultrasonic anemometer. For example, compare the first 15 s of trace a to trace b in figure 11. The second irregularity seems to be the ability of the propeller anemometer to follow updrafts better than downdrafts, as indicated in the last 15 s of the traces a and b in figure 10.

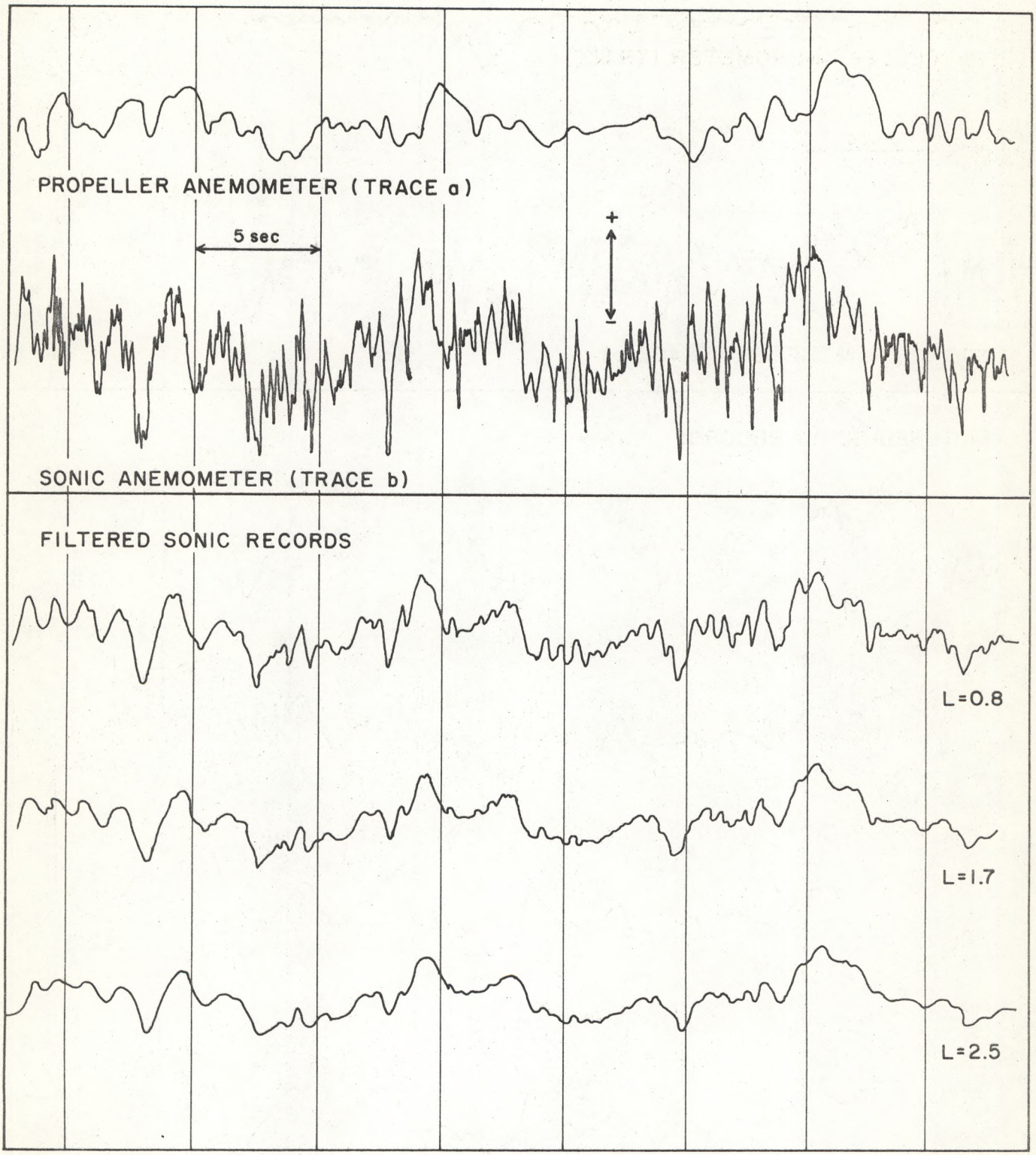

Figure 10. Strip-chart playbacks of ultrasonic anemometer records and corresponding Thornthwaite vertical propeller traces for a portion of run 58 B.

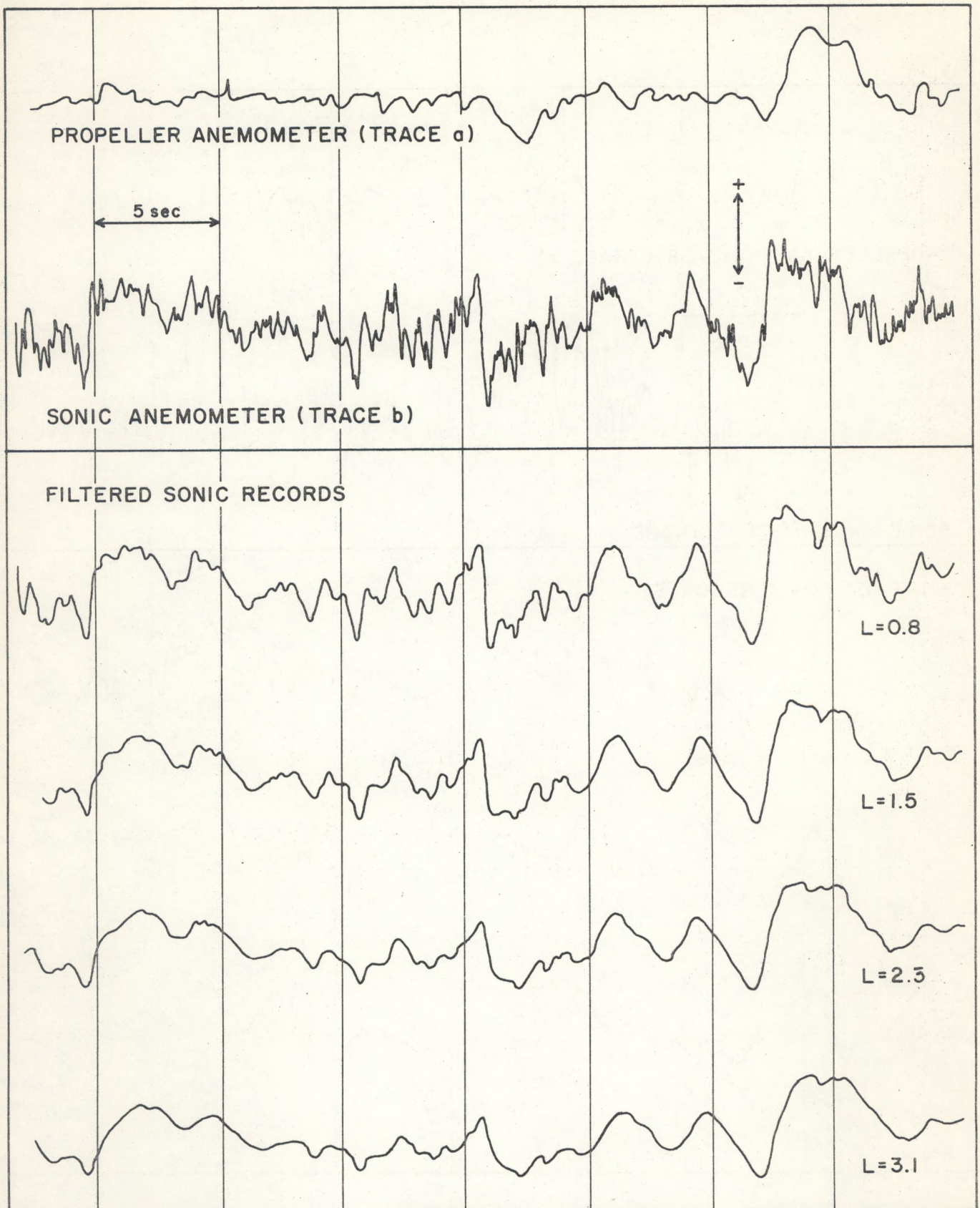

Figure 11. Strip-chart playback of ultrasonic anemometer records and corresponding Thornthwaite vertical propeller traces for a portion of run 58 C.

6.0 SUMMARY AND CONCLUSION

The standard deviations of the vertical wind component as measured by an ultrasonic anemometer were found to be consistent with measurements by other investigators, in that $\sigma/U = 0.09$. A negative 5/3 power law was found in the high frequency ($f > 1$; $f = nz/U$) spectral density estimates for almost all runs made at 2 m or above. In most cases a small positive skewness and kurtosis were computed, but when the low frequency fluctuations were filtered from the data the skewness values decreased while the kurtosis estimates increased, in some cases by more than a factor of 4. Spectral density estimates in the region of 3.5 Hz were used to estimate, on the basis of Kolmogorov's hypothesis, the rate of kinetic energy dissipation, the values of which decreased with height and increased with wind speed as found earlier by Ball (1961). Friction velocities were computed from three relationships that assume neutral conditions: the vertical kinetic energy budget, the wind profile, and an empirical relationship ($u = .77\sigma$). The best agreement was found between the first and third methods. The profile method overestimated the friction velocity in most cases.

Wind statistics from two ultrasonic anemometer arrays placed side by side were found to agree within the limits of the calibration ($\sim$ 6 percent). At a height of 1.6 m, an insignificant change in the standard deviation of the vertical wind component was observed after the wind had passed from smooth to tall grass over a 15-m fetch. Runs at four levels above the cut region show a consistent spectral shift to low frequency with increasing heights. No particular indication of the internal boundary layer between the rough and smooth grass flows was observed in the turbulent flow statistics.

Smoothed renderings of the ultrasonic anemometer records were found to resemble the Thornthwaite propeller anemometer output. When a series of filters were used to produce sonic traces of differing "distance constants," the propeller anemometer records seemed to fit between the traces with equivalent distance constants of 1.7 and 2.3 m.

7.0 ACKNOWLEDGMENTS

For extensive help in data gathering, we express our thanks to the staff of C. W. Thornthwaite Associates of New Jersey, in particular to Mr. William Superior. For assistance in the analysis, our thanks to Dr. Joshua Holland of the Atomic Energy Commission for the use of computer codes, and to Mrs. Doris Gordon and Mr. Anthony Giarrusso for processing the data, through these and other codes. This research has been supported by the Division of Reactor Development and Technology, U. S. Atomic Energy Commission.

8.0 REFERENCES

Ball, F. K. (1961), Viscous dissipation in the atmosphere, J. Meteorol. 18, No. 4, 553-557.

Batchelor, G. K. (1953), The Theory of Homogeneous Turbulence, 195 (Cambridge Univ. Press, London).

Blackadar, A. K., H. A. Panofsky, P. E. Glass, and J. F. Boogaard (1967), Determination of the effect of roughness change on the wind profile, Phys. Fluids, Suppl. 10, No. 9, S209.

Blackman, R. B., J. W. Tukey (1958) The Measurement of Power Spectra, 190 (Dover Publishing, Inc., N. Y.).

Busch, N. E. and H. A. Panofsky (1968), Recent spectra of atmospheric turbulence, Quart. J. Roy. Meteorol. Soc. 94, No. 400. 132-148.

Deacon, E. L. (1959), The problem of atmospheric diffusion, Intern. J. Air Pollution, 2, No. 2, 92.

Gibson, M. M. (1963), Spectra of turbulence in a rounded jet, J. Fluid Mech. 15, Pt. 2, 161.

Gurvich, A. S. (1960), Frequency spectra and functions of distributions of probabilities of vertical wind velocity components, Akademiia nauk SSSR. Izvestiia. Geophys. Ser., 1042-1055.

Gurvich, A. S. (1966), Probability distribution of the square of the velocity differential in a turbulent flow, Akademiia nauk SSSR. Izvestiia. Atmosph. and Ocean. Phy., 2, No. 10, 1095-1098.

Kaimal, J. C. (1963), A simplified sonic anemometer for measuring the vertical component of wind velocity, Report No. AFCRL-63-203, Air Force Cambridge Res. Labs., Bedford, Mass., 153 pp.

Kaimal, J. C. (1966), An analysis of sonic anemometer measurements from the Cedar Hill tower, Report No. AFCRL-66-542, Air Force Cambridge Res. Labs., Bedford, Mass., 153 pp.

Kistler, A. L. and T. Vrebalovich (1966), Grid turbulence at large Reynolds numbers, J. Fluid Mech. 26, No. 1, 37.

Kolmogorov, A. N. (1941), The local structure of turbulence in incompressible viscous fluid for very large Reynolds numbers. Akademiia nauk SSSR. Doklady. Series, 30, 301.

Lumley, J. L., and H. A. Panofsky (1964) The Structure of Atmospheric Turbulence (J. Wiley and Sons, N. Y.), 239 pp.

MacCready, P. B., Jr. (1962), The inertial subrange of atmospheric turbulence, J. Geophys. Res. 10, 1051.

MacCready, P. B., Jr., and H. R. Jex (1964), Response characteristics and meteorological utilization of propeller and vane wind sensors, J. Appl. Meteorol. 3, No. 2, 182-193.

Maitania, T. and Y. Mitsuta (1967), A direct measurement of vertical transport of turbulent kinetic energy in the air layer near the ground with sonic anemometers, Special Contribution, Geophys. Inst., Kyoto Univ., No. 7, 71-81.

Mitsuta, Y. (1966), Sonic anemometer-thermometer for general use, J. Meteorol. Soc. Japan, Ser. 2, 44, 12-24.

Panofsky, H. A. and R. A. McCormick (1960), The spectrum of vertical velocity near the surface, Quart. J. Roy. Meteorol. Soc. 86, No. 370, 494-503.

Pasquill, F. (1962), Atmospheric Diffusion, 297 (Van Nostrand, N. Y.).

Pond, S., S. D. Smith, P. F. Hamblin, and R. W. Burling (1966), Spectra of velocity and temperature fluctuations in the atmospheric boundary layer over the sea, J. Atmospheric Sci. 23, 376.

Pond, S. and R. W. Stewart (1965), Measurements of the statistical characteristics of small-scale turbulent motions, Akademiia nauk SSSR. Izvestiia Atmosph. and Ocean. Phys. 1, No. 9, 914-919.

Pond, S., R. W. Stewart, and R. W. Burling (1963), Turbulence spectra in the wind over waves, J. Atmospheric Sci. 20, 319.

Priestley, J. T. (1965), Correlation studies of pressure fluctuations on the ground beneath a turbulent boundary layer, National Bureau of Standards Report No. 8942, 92 pp.

Thornthwaite, C. W., W. J. Superior, J. R. Mather and F. K. Hare (1961), The measurement of vertical winds and momentum flux, C. W. Thornthwaite Assoc. Publications in Climatology XIV, No. 1, 89 pp.

APPENDIX

This appendix contains a listing of the spectral densities for all the rapid-response ultrasonic anemometer data collected during this experiment. All spectral densities are computed for a frequency resolution of 10^{-2} Hz, but they are tabulated in units of Hz^{-1}. All estimates are divided by the variance of the run, listed in table 2. Values written as 1.17-1 are to be interpreted as 1.17×10^{-1} Hz^{-1}.

Spectral Density Estimates $S(n)/\overline{(w')^2}$

Frequency	50 A	50 B	52	54	56	58 A	58 B	58 C	60 A-2	60 A-3	60 B-2	60 B-3
.01	5.07-0	5.5.-0	4.52-0	9.23-1	8.20-1	3.08-0	2.49-0	6.82-0	3.62-0	4.15-0	6.33-0	5.36-0
.02	4.60-0	6.43-0	5.63-0	1.19-0	9.97-1	2.96-0	2.14-0	5.13-0	3.52-0	2.28-0	3.82-0	2.59-0
.03	5.07-0	5.46-0	3.41-0	1.44-0	1.26-0	2.67-0	2.12-0	3.71-0	2.29-0	1.45-0	2.34-0	1.97-0
.04	3.40-0	3.56-0	3.04-0	1.25-0	1.75-0	1.98-0	1.63-0	2.60-0	2.09-0	1.65-0	2.40-0	2.16-0
.05	2.79-0	3.24-0	3.87-0	7.29-1	1.39-0	1.89-0	2.24-0	3.00-0	2.61-0	2.32-0	2.62-0	2.10-0
.06	2.98-0	3.52-0	2.37-0	1.61-0	7.45-1	1.86-0	2.29-0	3.25-0	2.00-0	2.51-0	1.17-0	1.77-0
.08	2.72-0	1.86-0	1.86-0	2.22-0	9.41-1	1.25-0	2.18-0	2.14-0	2.65-0	1.37-0	3.41-0	8.46-1
.1	1.23-0	1.36-0	1.25-0	1.04-0	9.62-1	1.16-0	1.03-0	1.58-0	1.93-0	1.53-0	2.00-0	1.07-0
.12	1.43-0	1.36-0	1.68-0	2.13-0	7.12-1	1.08-0	1.49-0	2.23-0	2.71-0	1.09-0	8.93-1	1.04-0
.15	1.18-0	7.55-1	7.99-1	8.36-1	7.15-1	1.37-0	1.24-0	1.63-0	6.81-1	8.42-1	1.79-0	1.72-0
.2	1.32-0	9.34-1	1.21-0	9.31-1	5.53-1	8.17-1	9.67-1	1.37-0	1.22-0	9.29-1	1.31-0	1.40-0
.3	6.66-1	7.23-1	7.39-1	1.01-0	4.56-1	9.44-1	8.05-1	7.85-1	7.76-1	5.75-1	9.52-1	6.84-1
.4	5.24-1	5.84-1	5.86-1	7.27-1	5.00-1	6.03-1	6.31-1	5.44-1	4.92-1	6.22-1	6.02-1	5.13-1
.5	5.43-1	4.89-1	5.06-1	5.62-1	4.75-1	5.68-1	4.95-1	3.96-1	4.21-1	5.56-1	4.29-1	4.38-1

Spectral Density Estimates $S(n)/\overline{(w')^2}$ (Continued)

Frequency	50 A	50 B	52	54	56	58 A	58 B	58 C	60 A-2	60 A-3	60 B-2	60 B-3
.6	4.00-1	3.36-1	3.94-1	5.24-1	4.08-1	4.52-1	4.28-1	3.18-1	4.16-1	4.59-1	4.36-1	3.98-1
.8	2.39-1	2.29-1	2.45-1	3.24-1	3.70-1	3.20-1	3.19-1	1.94-1	2.93-1	3.59-1	2.15-1	3.07-1
1.0	1.77-1	1.68-1	1.67-1	2.72-1	2.84-1	2.42-1	2.39-1	1.79-1	2.06-1	2.39-1	1.66-1	1.94-1
1.2	1.16-1	1.40-1	1.53-1	2.16-1	2.81-1	1.96-1	2.26-1	1.25-1	1.69-1	1.83-1	1.06-1	1.56-1
1.5	9.35-2	1.05-1	1.20-1	1.66-1	2.24-1	1.69-1	1.66-1	9.00-2	1.27-1	1.48-1	9.40-2	1.36-1
2.0	5.55-2	6.55-2	7.97-2	1.02-1	1.66-1	1.23-1	1.03-1	5.92-2	8.39-2	1.02-1	5.88-2	9.36-2
3.0	2.79-2	3.03-2	3.72-2	5.33-2	9.91-2	5.74-2	4.86-2	2.13-2	4.34-2	5.24-2	2.94-2	5.46-2
4.0	1.90-2	2.01-2	2.12-2	2.96-2	6.39-2	3.22-2	3.10-2	1.23-2	2.18-2	3.12-2	1.70-2	2.96-2
5.0	1.23-2	1.30-2	1.60-2	2.22-2	4.79-2	2.15-2	1.81-2	7.30-3	1.59-2	2.01-2	1.07-2	2.16-2
6.0	1.01-2	1.05-2	1.20-2	1.70-2	3.89-2	1.56-2	1.44-2	5.82-3	1.22-2	1.63-2	8.44-3	1.58-2
7.0	8.53-3	1.12-2	9.70-3	1.37-2	3.23-2	1.46-2	1.32-2	5.00-3	1.00-2	1.26-2	6.90-3	1.20-2
8.0				4.32-3	9.30-3	2.20-3	1.67-3			1.27-3		4.62-4

Spectral Density Estimates $S(n)/\overline{(w')^2}$ (Continued)

Frequency	62-2	62-3	64-2	64-3	66-2	66-3	68-2	68-3	70-2	70-3
.01	8.92-0	4.83-0	5.93-0	2.68-0	7.05-0	7.28-0	4.15-0	9.02-0	3.09-0	1.72-0
.02	6.25-0	1.92-0	6.79-0	2.38-0	6.38-0	2.17-0	3.66-0	2.74-0	2.38-0	1.83-0
.03	4.86-0	1.48-0	5.48-0	1.84-0	4.51-0	2.51-0	3.99-0	1.60-0	2.88-0	2.21-0
.04	3.78-0	1.01-0	5.49-0	2.07-0	3.80-0	2.15-0	3.47-0	1.74-0	3.16-0	3.48-0
.05	2.71-0	8.98-1	5.03-0	2.16-0	3.62-0	1.52-0	2.90-0	1.22-0	2.95-0	3.02-0
.06	2.17-0	1.33-0	3.36-0	2.01-0	3.08-0	1.82-0	3.64-0	1.38-0	1.75-0	1.72-0
.08	2.89-0	8.64-1	2.28-0	1.46-0	3.10-0	1.56-0	1.95-0	8.75-1	1.89-0	1.51-0
.1	1.92-0	9.13-1	1.43-0	1.13-0	1.48-0	1.27-0	1.67-0	9.22-1	1.44-0	1.38-0
.12	2.02-0	1.03-0	2.02-0	1.53-0	1.98-0	1.70-0	2.45-0	1.08-0	1.20-0	9.41-1
.15	1.27-0	5.10-1	1.58-0	1.32-0	1.68-0	1.05-0	9.94-1	8.12-1	7.21-1	6.70-1
.2	1.15-0	7.50-1	1.24-0	1.05-0	1.22-0	1.04-0	9.16-1	5.80-1	8.40-1	7.66-1
.3	7.82-1	6.00-1	8.09-1	7.76-1	7.96-1	5.70-1	7.64-1	4.64-1	4.40-1	5.14-1
.4	5.34-1	5.09-1	5.38-1	6.26-1	5.20-1	5.42-1	5.80-1	4.88-1	5.05-1	5.23-1
.5	3.83-1	4.35-1	3.32-1	5.29-1	3.77-1	5.17-1	4.73-1	4.31-1	4.79-1	4.48-1
.6	2.86-1	4.03-1	2.57-1	4.43-1	2.91-1	4.48-1	3.98-1	3.18-1	4.59-1	4.23-1

Spectral Density Estimates $S(n)/\overline{(w')^2}$ (Continued)

Frequency	62-2	62-3	64-2	64-3	66-2	66-3	68-2	68-3	70-2	70-3
.8	1.93-1	3.69-1	1.75-1	3.16-1	1.91-1	2.61-1	2.48-1	2.50-1	3.16-1	3.26-1
1.0	1.18-1	2.80-1	1.30-1	2.56-1	1.35-1	2.00-1	1.86-1	2.18-1	2.90-1	2.01-1
1.2	1.00-1	2.19-1	9.14-2	1.99-1	9.21-2	1.57-1	1.42-1	1.85-1	1.75-1	1.87-1
1.5	7.20-2	1.79-1	6.75-2	1.58-1	7.36-2	1.29-1	1.20-1	1.54-1	1.65-1	1.78-1
2.0	4.06-2	1.26-1	3.87-2	9.02-2	4.34-2	8.24-2	7.20-2	1.14-1	1.05-1	1.17-1
3.0	1.90-2	7.36-2	1.86-2	5.37-2	2.02-2	3.96-2	3.62-2	7.04-2	5.30-2	6.60-2
4.0	1.02-2	4.96-2	1.09-2	3.07-2	1.14-2	2.38-2	2.26-2	4.78-2	3.28-2	3.74-2
5.0	7.34-3	3.60-2	7.49-3	2.18-2	8.14-3	1.64-2	1.49-2	3.74-2	2.16-2	3.18-2
6.0	5.44-3	2.74-2	5.39-3	1.69-2	6.56-3	1.30-2	1.15-2	3.02-2	1.82-2	3.24-2
7.0	4.80-3	2.76-2	4.71-3	1.48-2	5.54-3	1.10-2	1.05-2	3.28-2	1.63-2	2.66-2
8.0		5.74-3		2.63-3				5.12-2	2.20-3	7.86-3